

Evaluation of microphone array methods for aircraft flyover measurements: Quantification of performance through virtual test environments

Timo Schumacher¹, Dorothea Lincke², Henri Siller³

¹ *TU Berlin, Fachgebiet Turbomaschinen- und Thermoakustik, 10623 Berlin, Germany, Email: t.schumacher@tu-berlin.de*

² *Empa, Swiss Federal Laboratories for Material Science and Technology, 8600 Dübendorf, Switzerland*

³ *Deutsches Zentrum für Luft- und Raumfahrt, 10623 Berlin, Germany*

Introduction

For the research and development of quiet aircraft technology, flyover measurements are used for the analysis of acoustic sources present in flight. When conducting those measurements with a phased microphone array, sources can be localized and separated, which allows the assessment of each aircraft components contribution to the total noise emitted. This detailed knowledge of the sources can be used e.g. for the acoustic evaluation of design choices.

The German Aerospace Center (DLR) has been developing microphone array techniques for flyovers since 1997 [1] and has continued to improve their ability throughout the years. This includes both the acquisition of the microphone signals as well as the following algorithms that calculate a source distribution.



Figure 1: The Aircraft ATRA (A320) has repeatedly been used for flyover measurements with a microphone array [2].

Motivation

When working with microphone data there are a number of algorithms available, each of which come with possible adjustments to choose from. Any alteration of an established process chain like the one described needs to be assessed. So far this has been done by comparing source maps like fig. 4 visually. This involved comparing the located source position with the position of expected sources, e.g. the engines or landing gear. As there are source maps for the emission angles (usually 3) as well as each third octave band, this can be quite tedious. Since it also is not systematic, there is room for interpretation which causes the evaluation to be subjective. Also, while the general layout of acoustic sources can be estimated beforehand, the exact location is unknown for real flyover measurements.

The virtual test cases which are described in the asso-

ciated paper "Evaluation of Microphone Array Methods for Aircraft Flyover Measurements: Development of a Virtual Test Environment" [3], aim to avoid this shortcoming. The exact position and power of each source is known and can be used to assess the quality of the localization result. Furthermore, this work aims to provide a method to quantify the quality without inspecting source maps directly.

Aircraft Flyover Measurements General Properties

While phased microphone array measurements are versatile and are used in many different contexts, flyover measurements in particular have some properties that need to be considered. In this paper, these properties will be highlighted. Where magnitudes are provided, they refer to measurement campaigns by the DLR in general, example values are taken from the 2016 LNATRA Campaign specifically [2].

When conducting flyovers, the altitude of the aircraft i.e. the distance to the microphone array is subject to constraints and cannot be freely chosen. It is generally large compared to other microphone array setups. In 2016, an altitude of between 180 m to 200 m was targeted. The speed during the flyover can differ for different test points which, depending on the required operating point, can represent a take-off, a landing or the approach and commonly lies within 60 m/s and 100 m/s. This corresponds with a high Mach number of up to 0.3. High speeds do not only cause challenging propagation effects due to the Doppler effect but also limit the length of the available time signals significantly.

In flyover measurements, the environmental conditions cannot be closely controlled. Wind can be measured only at ground level and at the aircraft itself, other motion of the propagating air due to atmospheric turbulences are unknown as a whole.

The great distance between array and sources, the high velocity, short time signals as well as uncontrollable and partially unknown environmental conditions create great challenges for microphone array techniques. This makes it reasonable to address them separately to other settings where microphone array techniques are applied.

Array Properties

When creating and evaluating a virtual test case, it is beneficial to use a similar process chain to when actual measurements are evaluated. The common procedure

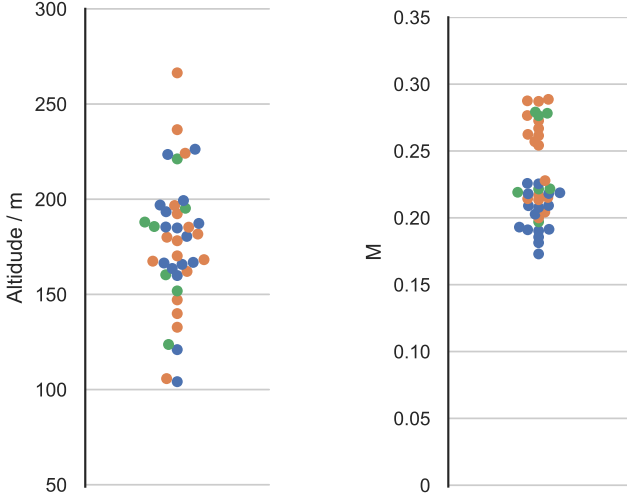


Figure 2: Measured altitude and Mach Number of the 2016 Campaign of some of the flyovers. The color represents the type of the operating point. Take-Off (●), Approach (●) and Landing (●)

within the DLR will be outlined in this section, again with the specifics taken from the campaign in 2016.

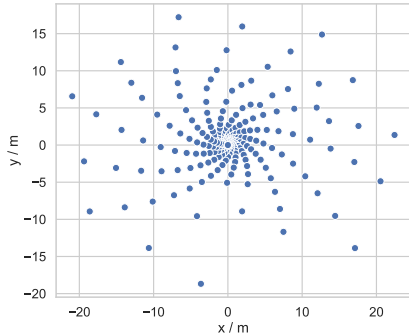
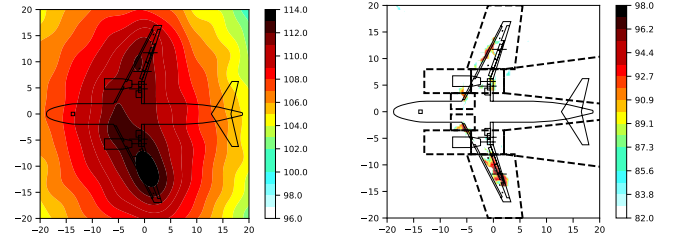


Figure 3: The 238 microphones of the array are arranged in a logarithmic spiral, with a diameter of 40 m.

The large microphone array used by the DLR contains 238 microphones, arranged in a logarithmic spiral (see fig. 3). The total diameter of the array, which is relevant for locating sources at low frequencies, is 40 m. The minimum distance of 12 cm between microphones is assumed at the center and is important for the localization of high frequency sources.

To render a good resolution for low as well as high frequencies, the arrays properties can be adapted for different frequency ranges. This can be accomplished by excluding some of the microphones and only using the remaining subarrays in the evaluation as in [5]. Alternatively one uses all signals, but their contribution to the result is set by a weighting factor depending on the microphones position. This is also known as shading [4]. Both methods have in common that they emphasize outer and



(a) Classical Sum-and-Delay source map

(b) Sum-and-Delay with additional deconvolution

Figure 4: Resulting source maps of a flyover measurement. $f = 500$ Hz

suppress inner microphones for low frequencies and invert this scheme for high frequencies. For this study, the latter approach is chosen. The used weighting factors are based on works by [6] and invert the mentioned strategy at around 1000 Hz to 1250 Hz.

Definition of Metric

With a set of isolated sources, a good localization result detects a source amplitude only on grid points close to those sources and is zero, or close to zero, otherwise. One can define a region surrounding the expected source positions and integrate the intensity of the source within this region. Putting this value in relation to the total source intensity of the map, one obtains a ratio between zero and one. Here, values close to one are desirable and show that the sources were located correctly.

$$\text{Metric} := \frac{\text{Source intensity within defined region}}{\text{Total intensity of the map}} \quad (1)$$

A similar approach, but for measured data, is described in [5].

The size and shape of the region surrounding the source locations can be selected arbitrarily. Here a rectangular shape parameterized by a diameter D is used, where the rectangle extends a distance of $D/2$ in each direction. We propose altering this value to obtain additional information about the distribution of the located sources.

Figure 6 depicts the metric for a range of different diameters D and Third Octave Bands, with nominal frequency $f_{nom} = 80, 100, 125, \dots, 8000$. The corresponding source maps with the different integration regions are shown in fig. 5.

Interpretation

This representation of the metric value enables a quick assessment across all frequencies how close the resulting sources are located to the real source position. For a classical beamforming source map, fig. 6 is as expected: For a fixed frequency, the metric value increases gradually. This is due to the convolution of the acoustic sources with the point spread function, which is an inherent effect of classical Delay-and-Sum beamforming. This effect is increased for low frequencies where the main lobe of the point spread function has a high beam width (see fig. 4).

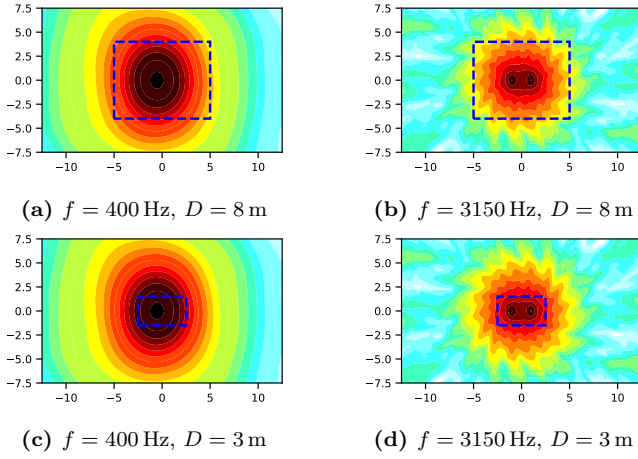


Figure 5: Source maps for a virtual test case with two sources in the center, 2 m apart. The region for integration are marked by the dotted line. The proposed metric yields 0.35, 0.75, 0.08 and 0.36 respectively, confirming that the classical beamforming yields worse spatial resolution for low frequencies.

Results that were computed with different approaches or a different parametrization can be compared by simply subtracting the metric values from one another. This is demonstrated in figs. 7 and 8. Here each microphone contributes equally (fig. 7a) and where microphones are weighted according to their position (fig. 7b). The difference in fig. 7c shows, that almost everywhere the usage of the shading approach factors improves the Sum-and-Delay beamforming results.

The proposed metric with the corresponding representation by heat maps can easily be used on all types of source maps independently of the method they are based on. An example is provided in fig. 8, where additionally to the beamforming a deconvolution approach has been used, again with and without shading. The comparison in fig. 8c clearly shows that the usage of shading is still beneficial, though the advantage is not as big as in the case of beamforming by itself.

Conclusion

A system has been developed and presented that allows a quick assessment of the quality of source localization results. It relies on virtual test cases that reproduce realistic microphone array signals. This way, they can be processed similar to real data, but the desired output is known in advance. The defined metric is straightforward. This provides robustness and versatility to the scope of application. Altering the region size and displaying the resulting values we created a plot that densely but accessibly provides information about the quality of the method.

We have demonstrated that one is able to compare similarly shaped sourcemap results based on identical microphone array data. The effect of changed parameters or methods to a evaluation can be easily studied. So far, it is not able to provide a global rating for array methods that can be easily transferred to other contexts. Also,

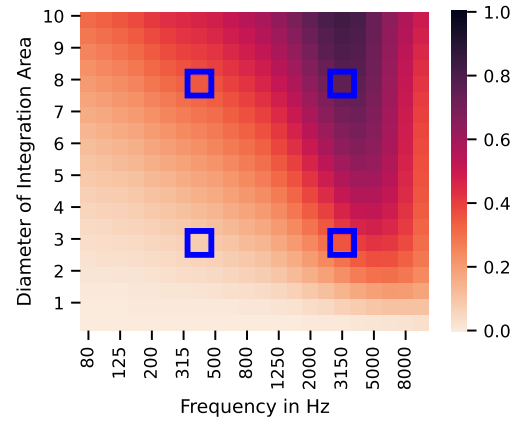


Figure 6: Heat map representation for the metric values for different diameters D and frequencies f . This plot corresponds to the source maps presented in fig. 5, with the blue markers pointing to the positions of the fig. 5 (a), (b), (c) and (d) in the same arrangement as in the figure.

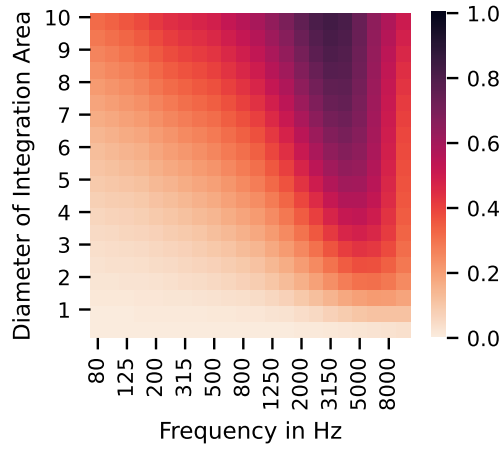
while being a good measure for the correct localization of sources, it does not provide information about other characteristics necessary to determine the quality of a method, e.g. insensitivity to disturbed microphone signals, source separation. The enhancement of the meaningfulness by including noisy or partially decorrelated signals is subject to further works. A main goal must be to do so while keeping the approach simple to interpret.

Funding

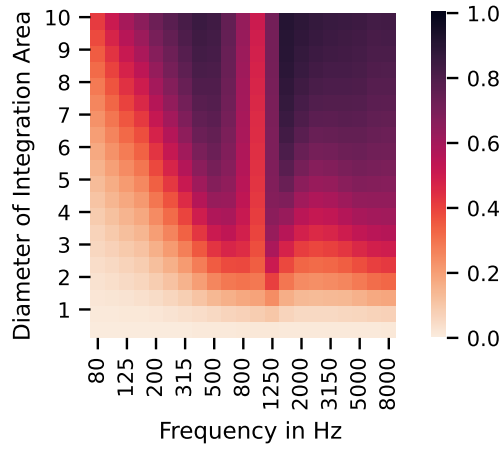
This work is part of the international research project Localization and Identification Of moving Noise sources (LION). The German contribution is funded by the Deutsche Forschungsgemeinschaft (DFG).

References

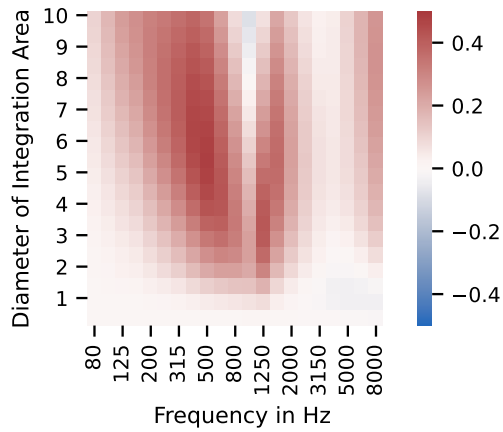
- [1] Michel, U. et al.: Investigation of airframe and jet noise in high-speed flight with a microphone array. 3rd AIAA/CEAS Aeroacoustics Conference (1997)
- [2] Siller, H. et al.: Source localisation on aircraft in flight - new measurements with the dlr research aircraft airbus 320 atra. 7th BeBeC (2018)
- [3] Lincke et al.: Evaluation of Microphone Array Methods for Aircraft Flyover Measurements: Development of a Virtual Test Environment. DAGA22 (2022)
- [4] Johnson, D.H. and Dudgeon, D.E.: Array Signal Processing: Concepts and Techniques. Prentice Hall, 1993
- [5] Brusniak, Leon et al.: Acoustic Phased Array Quantification of Quiet Technology Demonstrator 3 Advanced Inlet Liner Noise Component. 25th AIAA/CEAS Aeroacoustics Conference (2019)
- [6] Guérin, S. et al.: Beamforming and deconvolution for aerodynamic sound sources in motion. 1st Berlin Beamforming Conference (2006)



(a) No shading

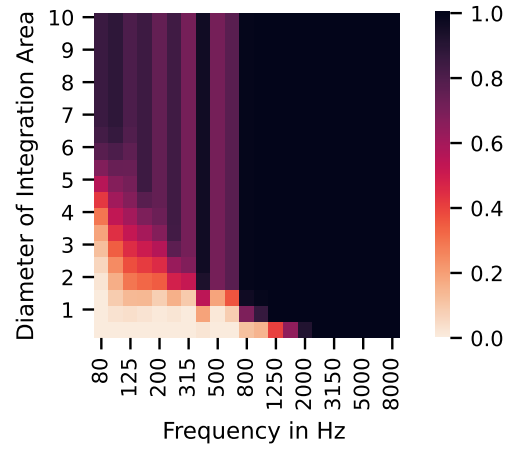


(b) Shading active

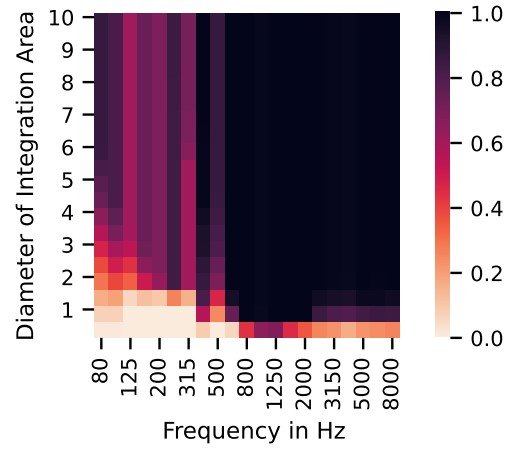


(c) Difference in value

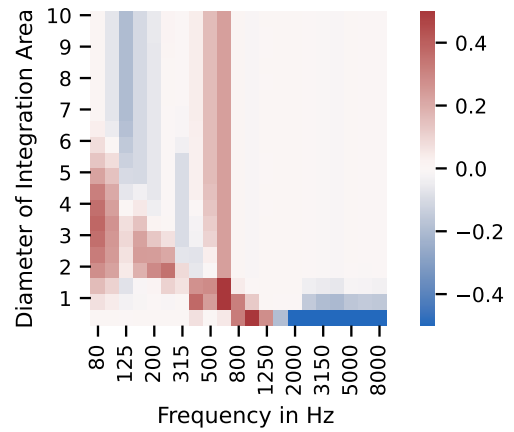
Figure 7: Metric plots for classical beamforming results without and with a weighting of the microphones active. (c) displays the difference, with positive values showing a advantage of activated shading $(c) = (b)-(a)$.



(a) No shading



(b) Shading active



(c) Difference in value

Figure 8: Metric plots for deconvolution results without and with a weighting of the microphones active. (c) displays the difference, with positive values showing a advantage of activated shading $(c) = (b)-(a)$.